

5T4 Glycoprotein Regulates the Sensory Input-Dependent Development of a Specific Subtype of Newborn Interneurons in the Mouse Olfactory Bulb

Sei-ichi Yoshihara,¹ Hiroo Takahashi,¹ Nobushiro Nishimura,¹ Hiromi Naritsuka,² Taichi Shirao,³ Hirokazu Hirai,⁴ Yoshihiro Yoshihara,⁵ Kensaku Mori,² Peter L. Stern,⁶ and Akio Tsuboi¹

¹Laboratory for Molecular Biology of Neural System, Advanced Medical Research Center, Nara Medical University, 840 Shijo-cho, Kashihara, Nara 634-8521, Japan, ²Department of Physiology, Graduate School of Medicine, University of Tokyo, Tokyo 113-0033, Japan, ³Nikon Instech Company, Ltd., Tokyo 100-0006, Japan, ⁴Department of Neurophysiology, Gunma University Graduate School of Medicine, Gunma 371-8511, Japan, ⁵Laboratory for Neurobiology of Synapse, RIKEN Brain Science Institute, Saitama 351-0198, Japan, and ⁶Cancer Research UK Immunology Group, Paterson Institute for Cancer Research, University of Manchester, Manchester M20 4BX, United Kingdom

Sensory input has been shown to regulate development in a variety of species and in various structures, including the retina, cortex, and olfactory bulb (OB). Within the mammalian OB specifically, the development of dendrites in mitral/tufted cells is well known to be odor-evoked activity dependent. However, little is known about the developmental role of sensory input in the other major OB population of the GABAergic interneurons, such as granule cells and periglomerular cells. Here, we identified, with DNA microarray and *in situ* hybridization screenings, a trophoblast glycoprotein gene, *5T4*, whose expression in a specific subtype of OB interneurons is dependent on sensory input. *5T4* is a type I membrane protein, whose extracellular domain contains seven leucine-rich repeats (LRR) flanked by characteristic LRR-N-flanking and C-flanking regions, and a cytoplasmic domain. *5T4* overexpression in the newborn OB interneurons facilitated their dendritic arborization even under the sensory input-deprived condition. By contrast, both *5T4* knockdown with RNAi and *5T4* knockout with mice resulted in a significant reduction in the dendritic arborization of *5T4*⁺ granule cells. Further, we identified the amino acid sequence in the *5T4* cytoplasmic domain that is necessary and sufficient for the sensory input-dependent dendritic shaping of specific neuronal subtypes in the OB. Thus, these results demonstrate that *5T4* glycoprotein contributes in the regulation of activity-dependent dendritic development of interneurons and the formation of functional neural circuitry in the OB.

Introduction

Neural circuitry is adjusted by sensory input from the external world in postnatal stages. Olfactory bulb (OB) interneurons are a good model for studying neural circuit modification by the sensory experience (Katz and Shatz, 1996; Sanes and Lichtman,

2001; Nithianantharajah and Hannan, 2006). The OB interneurons are generated and integrated into the pre-existing neural circuit throughout life (Lledo et al., 2008; Whitman and Greer, 2009; Adam and Mizrahi, 2010; Kaneko et al., 2010; Sakamoto et al., 2011). Newborn interneurons are generated in the subventricular zone, migrate along the rostral migratory stream (RMS), and differentiate into GABAergic interneurons, such as granule cells (GCs) and periglomerular cells (PGCs) (Lledo et al., 2008; Whitman and Greer, 2009; Adam and Mizrahi, 2010; Kaneko et al., 2010; Sakamoto et al., 2011). It is known that odor-evoked activity affects the survival and integration of newborn OB interneurons (Rochefort et al., 2002; Yamaguchi and Mori, 2005; Lin et al., 2010). In addition, olfactory sensory deprivation or odor-rich environment can promote suppression or acceleration of both dendritic morphogenesis and spine formation of newborn OB interneurons, respectively (Saghateljan et al., 2005; Livneh et al., 2009). These results suggest that the odor-evoked activity facilitates the survival rate, dendritic morphogenesis, and spine formation of the OB interneurons. However, little is known about the molecular players or the precise mechanisms that integrate odor-evoked activity with the developmental processes of OB interneurons.

In this study, DNA microarray and *in situ* hybridization screenings in the unilaterally naris-occluded OB identified an

Received Nov. 28, 2011; accepted Dec. 20, 2011.

Author contributions: S.Y. and A.T. designed research; S.Y., H.T., N.N., H.N. and T.S. performed research; T.S., H.H., Y.Y., K.M., and P.L.S. contributed unpublished reagents/analytic tools; S.Y., H.T., N.N., and A.T. analyzed data; S.Y., P.L.S., and A.T. wrote the paper.

This work was supported by grants from Grant-in-Aid for Scientific Research for Basic Research (C) and Priority Areas (Cell Sensor) from the Ministry of Education, Culture, Sports, Science and Technology (MEXT), Japan. A.T. was supported by grants from Naito, Novartis, Terumo, Applied Enzymology, Urakami, Mishimakaiun Memorial, and Uehara Memorial Foundations, and Daiwa Housing Group (Indoor Environmental Medicine), Japan. S.Y. and H.T. were supported by a Grant-in-Aid for Young Scientists (B) from MEXT and a grant from the Kao Foundation for Arts and Sciences, Japan. S.Y. was supported by grants from Sumitomo, Mochida Memorial, Naito, Life Science, Cosme-tology, and Takeda Science Promotion Foundations, Japan. H.T. was supported by a Grant-in-Aid for Priority Areas (Neurovascular Network) from MEXT, and grants from Uehara Memorial and Inamori Foundations, Japan. P.L.S. was supported by funding from Cancer Research UK Grant C480/A12328. We gratefully thank H. Sakano for encouraging this study, and the staffs of the animal facility of Nara Medical University for expert assistance. We thank RIKEN BSI Research Resource Center for help in DNA microarray analysis. We gratefully thank the staff of the animal facility and Jian Li of Paterson Institute for Cancer Research for expert contributions.

Correspondence should be addressed to Akio Tsuboi, Laboratory for Molecular Biology of Neural System, Advanced Medical Research Center, Nara Medical University, 840 Shijo-cho, Kashihara, Nara 634–8521, Japan. E-mail: atsuboi@naramed-u.ac.jp.

DOI:10.1523/JNEUROSCI.5907-11.2012

Copyright © 2012 the authors 0270-6474/12/322217-10\$15.00/0

oncofetal glycoprotein gene, *5T4*, whose expression in the OB GCs is dependent on sensory input. *5T4* is a type I transmembrane (TM) protein, whose extracellular (EC) domain contains seven leucine-rich repeats (LRR) flanked by characteristic LRR-N-flanking and C-flanking regions, and a cytoplasmic domain with a PDZ interacting motif. *5T4* protein was first identified while searching for molecules with invasive properties likely to be shared by placental trophoblasts and cancer cells (Hole and Stern, 1990). *5T4* expression is upregulated in many different carcinomas, while showing only low levels in most normal tissues (Southall et al., 1990) except for high levels in brain and ovary (King et al., 1999; Barrow et al., 2005). The *5T4* overexpression in epithelial cells causes the disruption of cell–cell contacts, downregulation of E-cadherin (Carsberg et al., 1996), altered morphology, and increased cellular motility, while *5T4* upregulation associated with embryonic stem cell differentiation appears to be an integral component of epithelial-to-mesenchymal transition (Eastham et al., 2007; Spencer et al., 2007). Here, using a lentiviral system, providing either gain- or loss-of-function for *5T4* gene in the developmental processes of OB interneurons, plus *5T4* knock-out (KO) mice, we establish that *5T4* glycoprotein regulates the dendritic arborization of the $5T4^+$ GCs in a sensory input-dependent manner.

Materials and Methods

Mice and naris occlusion procedure. Animal research was approved by the campus committee of Nara Medical University and Paterson Institute for Cancer Research, University of Manchester, and was conducted in accordance with its guidelines. We used ICR male and female mice purchased from Japan SLC. Olfactory sensory deprivation was performed by the naris occlusion. Newborn mice at postnatal day 0 (P0) were anesthetized with ice, and then the unilateral nostril was cauterized by a soldering iron.

***5T4* knock-out mice.** We have constructed a *5T4* KO mouse line by replacing the second exon of *5T4*, which encodes the entire protein, with an *IRES-LacZneo* reporter gene in ES cells (Southgate et al., 2010). These cells were used to produce chimeric mice and germline progeny; *5T4* heterozygote mice were backcrossed to the C57BL/6 background. The *5T4* KO C57BL/6 animals are viable, but adult animals show some structural disorganization within the brain and exhibit a high frequency of hydrocephalus. The frequency of hydrocephalus is ~13%, with the median age of death at P49.

DNA microarray analysis. Total RNA was extracted separately from the open and closed sides of OB from three naris-occluded mice (P28). These total RNA samples were used as the probe templates of GeneChip Mouse Genome 430 2.0 DNA microarray (Affymetrix). The DNA microarray expression profiles were compared between the open and closed sides of OB. DNA microarray statistical analysis was performed as described previously (Inoue et al., 2004). The genes expressing a >1.5-fold change between the open and closed sides of OB were further analyzed by *in situ* hybridization.

Generation and injection of lentiviral vectors. Lentiviral vectors were provided kindly by Dr. Arthur Nienhuis (St. Jude Children's Research Hospital, Memphis, TN) and Dr. Hirokazu Hirai (Gunma University, Maebashi City, Japan). Recombinant lentiviral vectors, expressing the *gapEYFP*, *gapmCherry*, and *5T4-IRES-gapEYFP* genes under the control of the *CMV* or *5T4* promoter (6 kb), were prepared as described previously (Torashima et al., 2006). For *5T4* knockdown experiments, short hairpin RNAs (shRNAs) were expressed under the human *H1* promoter. Three sets of shRNAs targeted at the *5T4* gene were designed by siDirect version 2.0 (<http://sidirect2.rnai.jp/>). The following sets of shRNAs were cloned into the lentiviral vector: sh1, GGTA TCATTACAGATACGATTCAAGAGATCGTATCTGTAATGATACC CTTTTT; sh2, GACCTTGATCCTTGTTATGTATTCAAGAGATAC ATAACAAGGATCAAAGTCTTTTT; and sh3, GCTCTTACATAGAA CTTTGTATTCAAGAGATACAAAGTTCTATGTAAGAGCTTTTT.

Newborn mice (P0) were anesthetized with ice, and then 0.5 μ l of lentiviral vector was injected into the lateral ventricle by an Injection

Pump KDS 310 (KD Scientific). The titers of lentivirus were adjusted to 2.0×10^8 transducing units/ml.

In situ hybridization. The entire coding region of the *5T4* gene was used as the template of a digoxigenin (DIG)-labeled RNA probe. Naris-occluded ICR mice at 3 weeks postnatally (P21) were anesthetized with sodium pentobarbital (2.5 mg/animal) and perfused intracardially with 4% paraformaldehyde (PFA). Mouse brains were dissected out and fixed in PBS containing 4% PFA on ice for 1 h. Tissues were placed for 1 d in 30% sucrose and embedded in O.C.T. compound (Tissue-Tek) in liquid nitrogen. Serial coronal sections (20 μ m) were cut with a JUNG CM1900 (Leica) and collected on 3-aminopropyl-triethoxysilane-coated slide glasses. The procedures used for hybridization, washings, and antibody reaction were done as described previously (Tsuboi et al., 1999). Slides were incubated with alkaline phosphatase-conjugated anti-DIG antibody (anti-DIG-AP; Roche Diagnostics), and positive cells were stained with NBT/BCIP (Roche Diagnostics) or HNPP Fluorescent Detection Set (Roche Diagnostics). Images were acquired using a BX50 microscope equipped with a CCD camera M3204C (Olympus) and processed by Adobe Photoshop. With the exception of minor adjustments in brightness and contrast, the images were not altered.

Immunohistochemistry. Immunohistochemistry (IHC) of the mouse OB sections was performed as described previously (Yoshihara et al., 2005). Primary antibodies used were as follows: rabbit anti-GFP (1:1000, Life Technologies); rat anti-GFP (1:1000, Nakalai Tesque); rabbit anti-RFP (1:1000, Clontech Laboratories); rat anti-RFP (1:1000, ChromoTek); rabbit anti-*5T4* antibody (1:1000) (Imamura et al., 2006); sheep anti-*5T4* (1:1000, R&D Systems); mouse anti-mouse *5T4* monoclonal antibody (1:1000) (Southgate et al., 2010); and chicken anti-lacZ (1:1000, Abcam). DyLight 488-, DyLight 549-, and DyLight 649-conjugated secondary antibodies were purchased from Jackson ImmunoResearch. In enhanced yellow fluorescent protein (EYFP) IHC, OB sections from ICR mice, where the *CMVp-5T4-IRES-gapEYFP* lentiviral vector was injected, was enhanced by tyramide signal amplification (TSA) method (PerkinElmer). TSA IHC of OB sections was performed with horseradish peroxidase-conjugated goat anti-rabbit IgG (H+L) (1:1000, Life Technologies), Alexa Fluor 488-conjugated streptavidin (1:500, Life Technologies), and TSA Biotin Tyramide reagent pack (PerkinElmer). DAPI nuclear counterstaining was performed on all OB sections. Images were acquired using IX71 microscope equipped with a CCD camera DP30BW (Olympus), a confocal laser microscope FV1000 (Olympus), and a multiphoton confocal laser microscope AIR MP (Nikon). Stacked images in the *x-y* plane from individual thin-sectioned slices were superimposed with Adobe Photoshop to reveal the entire morphology of cells.

Statistical analyses. Total length of dendrites and *5T4* hybridizing-signal intensities were analyzed with ImageJ software (National Institutes of Health). Total length of dendrites is the sum of all dendritic branches of a single neuron. A branching point is the point where a neurite extends from the cell body or from another neurite. A process has to be at least 10 μ m to be considered a branch. The branching number of dendrites is the sum of every branching point from a single neuron. All data were analyzed with Microsoft Excel 2007 using Student's *t* test. Descriptive statistics were displayed as the mean \pm SEM. Differences were deemed significant at $p < 0.05$.

Results

5T4 gene shows sensory input-dependent expression in a specific subtype of newborn OB interneurons

To test whether sensory input affects dendritogenesis of newborn mouse OB interneurons, a lentiviral vector, expressing the membrane-associating *gapEYFP* under the control of the *CMV* promoter (*CMVp-gapEYFP*), was injected into the lateral ventricles at P0 (Fig. 1A), followed by unilateral naris occlusion. After 3 weeks (P21), we analyzed the dendritogenesis of newborn OB interneurons by confocal microscopy (Fig. 1B,C) and two-photon microscopy (data not shown). We found the volumes of the external plexiform and GC layers were reduced in the closed side compared with the open side of OB, but variability in the numbers of EYFP⁺ interneurons in individual mice precluded

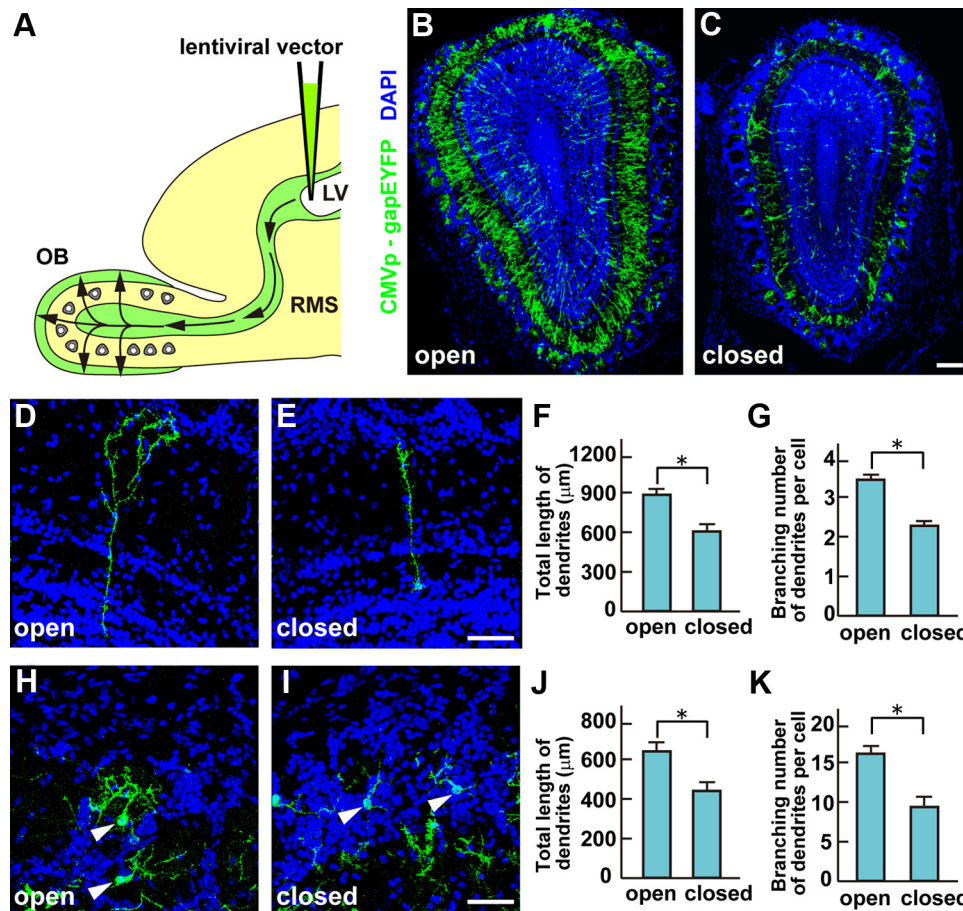


Figure 1. Sensory input is required for the dendritic elongation and arborization of newborn OB interneurons. *A*, Schematic diagram of the experimental protocol. A lentiviral vector carrying *CMVp-gapEYFP* was injected into the lateral ventricle (LV) of P0 mice. EYFP⁺ interneurons in OB were analyzed 3 weeks (P21) after injection. *B, C*, Newborn OB interneurons in the open (*B*) and closed (*C*) sides of OB from P21 naris-occluded mice, where the unilateral nostril was closed at P0. The volumes of external plexiform and granule cell layers were reduced on the closed side compared with the open side of OB. Scale bar, 100 μm . *D, E*, Newborn GCs in the open (*D*) and closed (*E*) sides of OB from P21 naris-occluded mice. Scale bar, 50 μm . *F, G*, Quantification on the total lengths (*F*) and the branching numbers (*G*) of GC dendrites is shown as the mean \pm SEM (*F*: open = $878 \pm 26 \mu\text{m}$, closed = $556 \pm 17 \mu\text{m}$; *G*: open = 3.4 ± 0.1 , closed = 2.5 ± 0.1 ; $*p < 0.01$ compared with the open side, Student's *t* test, $n = 50$ cells in each side of OB from three individuals). *H, I*, Newborn PGCs in the open (*H*) and closed (*I*) sides of OB from P21 naris-occluded mice. Scale bar, 50 μm . *J, K*, Quantification of the total lengths (*J*) and the branching numbers (*K*) of PGC dendrites is shown as mean values \pm SEM (*J*: open = $653 \pm 41 \mu\text{m}$, closed = $422 \pm 18 \mu\text{m}$; *K*: open = 17.2 ± 1.2 , closed = 8.5 ± 0.8 ; $*p < 0.01$ compared with the open side, Student's *t* test, $n = 50$ cells in each side of OB from three individuals). Newborn GCs and PGCs had a shorter length and fewer branched dendrites on the closed than the open side of OB.

conclusions about any reduction in numbers of newborn interneurons with naris closure. However, both measurements of the total length and the branching number of GC dendrites (Fig. 1*D–G*) from P21 naris-occluded mice showed that there was a 1.6- or 1.4-fold reduction, respectively, in the closed side compared with the open side of OB. We also observed that both the total length and branching number of PGC dendrites were reduced 1.5- and 2.0-fold in the closed side compared with the open side of OB, respectively (Fig. 1*H–K*). These results confirm that odor-evoked sensory input is necessary for dendritic elongation and arborization of interneurons of GCs and PGCs in OB (Saghatelian et al., 2005; Kelsch et al., 2009). To investigate the molecules regulating the development of OB interneurons, a DNA microarray approach was used.

A microarray analysis, searched for genes whose expression levels differed between the open and closed sides of OB but correlated with interneurons (data not shown), was assessed by *in situ* hybridization. Among 38 candidate genes, 5T4 oncofetal trophoblast glycoprotein showed clear differences in expression levels between the open and closed sides of OB (Fig. 2*A, B*). Interestingly, Imamura et al. (2006) reported that 5T4 is localized

in the dendrites of a specific subset of OB interneurons and is reduced in expression levels by olfactory deprivation. This suggested that 5T4 could be a factor regulating the dendritic arborization and synaptic connection of 5T4⁺ GCs, depending on the degree of sensory input. Thus, we chose the 5T4 gene for further analyses to confirm its expression in the OB and following naris occlusion. 5T4 was expressed in a specific subset of PGCs or GCs at the glomerular layer or at the mitral and superficial GC layers, respectively (Fig. 2*A, B*). In the olfactory-deprived OB, 5T4⁺ cell numbers were decreased 1.9-fold in the glomerular, mitral cell, and superficial GC layers (Fig. 2*A–C*). Moreover, the average fluorescent intensities of 5T4 hybridization signals were reduced 1.7-fold in the closed side compared with the open side of OB (Fig. 2*A, B, D*). These results demonstrate that 5T4 gene is expressed in the specific subtype of GCs, depending on the sensory input.

Overexpression of 5T4 facilitates the dendritic arborization of OB granule cells

Because 5T4 protein is localized preferentially at the GC dendrites in OB (Imamura et al., 2006), it is possible that 5T4 regulates the dendritogenesis or synaptogenesis of OB interneurons

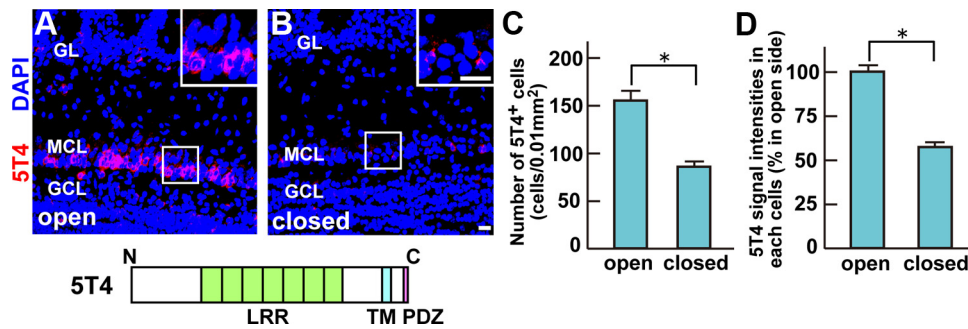


Figure 2. The *5T4* gene is expressed in a specific subtype of OB interneurons in a sensory input-dependent manner. **A, B**, Fluorescent *in situ* hybridization of OB sections from P21 naris-occluded mice. *5T4* hybridizing and DAPI staining signals are shown as red and blue, respectively. The *5T4* gene was expressed in a specific subset of PGCs and GCs. The *5T4*⁺ interneurons were located mainly in the mitral cell layer (MCL) and superficial granule cell layer (GCL), and slightly in the glomerular layer (GL). Insets show the enlarged image of the area enclosed with white squares. Scale bar, 20 μm . **C, D**, Quantification on cell numbers (**C**) and hybridizing signal intensities (**D**) of the *5T4*⁺ GCs, shown as the mean \pm SEM (**C**: open = 162 ± 24 cells/0.01 mm², closed = 86 ± 17 cells/0.01 mm²; **D**: open = $100 \pm 7\%$, closed = $58 \pm 5\%$; $*p < 0.01$ compared with the open side, Student's *t* test, $n = 50$ cells in each side of OB from three individuals). Both the *5T4*⁺ cell number and its expression level in each neuron were reduced on the closed side compared with the open side of OB.

following sensory input. To investigate the role of *5T4* in the neuronal development within OB, a gain-of-function experiment was performed by injecting a lentiviral vector that carries the *CMVp-5T4-IRES-gapEYFP* gene into the lateral ventricles of P0 mice. After 3 weeks (P21), the dendritogenesis of *5T4*-expressing neurons was compared with that of the control *EYFP*-expressing ones. Differences in the dendritic morphology between the control and the *5T4* overexpressing GCs were dependent on positions of the cell bodies in the layers. For example, in the mitral cell layer, *5T4*-overexpressing GCs had 2.6-fold more branched dendrites than those of the control *EYFP* (Fig. 3A–C), while in the GC layer they showed 1.5-fold more branched dendrites than the control *EYFP* (data not shown). *5T4* overexpression in adult GCs following infection into P56 mice gave similar results (a 3.1-fold increase in branching numbers) in those at newborn age (data not shown). These results demonstrate that the *5T4* gain-of-function facilitates the dendritic arborization of newborn GCs in the OB.

When the olfactory sensory input is deprived, both the total length and the branching numbers of GC dendrites are reduced (Fig. 1). We tested whether dendritic arborization could be restored by overexpression of *5T4* under the activity-reduced condition. This was achieved by coinjection of two lentiviral vectors (*CMVp-5T4-IRES-gapEYFP* and control *CMVp-gapmCherry*) into the lateral ventricles of P0 mice, followed by unilateral naris occlusion (Fig. 4A, B). As expected, after 2 weeks (P14), GCs expressing the control *mCherry* had 1.6-fold fewer branched dendrites on the closed than on the open side of OB (Fig. 4C, D, compare controls). Interestingly, GCs overexpressing the *5T4* gene in the mitral cell layer had 2.3- and 3.5-fold more branched dendrites in both the open and closed sides of OB, respectively (Fig. 4C, D). These results demonstrate that *5T4* overexpression facilitates the dendritic arborization of the OB interneurons including with olfactory deprivation.

5T4 intracellular domain is necessary and sufficient for the dendritic arborization

A series of lentiviral *5T4* deletion constructs were used to establish which domains of *5T4* are required for the dendritic ar-

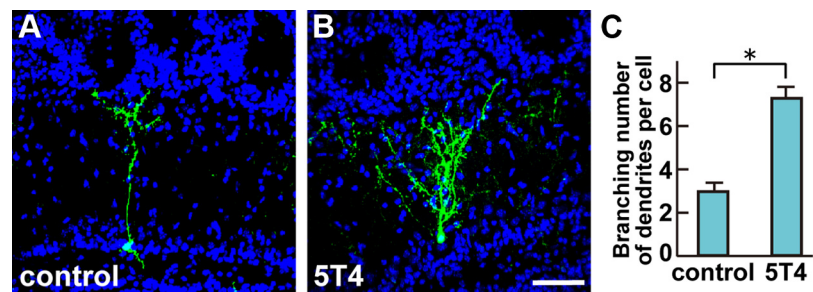


Figure 3. Gain-of-function of *5T4* facilitates the dendritic arborization of OB interneurons. **A, B**, Expression of a lentivirus carrying the control (*CMVp-gapEYFP*) (**A**) or *5T4* (*CMVp-5T4-IRES-gapEYFP*) vector (**B**) in the GCs from P14 mice. Scale bar, 50 μm . **C**, Quantification of branching numbers of the GC dendrites is shown as the mean \pm SEM (control = 2.8 ± 0.3 , *5T4* = 7.3 ± 0.3 , $*p < 0.01$ compared with the control, Student's *t* test, $n = 30$ cells in each line from three individuals). The *5T4*-overexpressing GCs had more branched dendrites than the control cells.

borization. Interestingly, overexpression of a construct deleting the LRRs of the extracellular domain (*5T4- Δ LRR*) gave 2.5-fold more branched dendrites in the GCs than the control *EYFP*-injected mice, similar to a 2.6-fold increase seen with the *5T4*-full length construct (Fig. 5B, C, E). By contrast, overexpression of the intracellular (IC) domain-deletion construct (*5T4- Δ IC*) showed a similar level (1.1-fold) of branching numbers in the GC dendrites to that of the control *EYFP* (Fig. 5A, D, E). To further map the specific sequence of the 44 aa cytoplasmic domain involved, lentiviral vectors with 10, 20, 30, and 40 aa deletions from the C terminus were generated and injected into P0 mice (Fig. 5B, F–J). Overexpression of the *5T4* C-terminal 10 aa deletion (*5T4- Δ C10*) gave 2.6-fold more branched dendrites in the GCs than that of the control *EYFP*, similar to a 2.6-fold increase seen with overexpression of the *5T4* full length construct (Fig. 5B, F, J). This *5T4- Δ C10* construct lacks the PDZ-binding motif (SDV), showing that it is not involved in the dendritic arborization of GCs. Expression of the *5T4* C-terminal 20 aa deletion (*5T4- Δ C20*) gave 1.5-fold more branching numbers in the GC dendrites than that of the control *EYFP* (Fig. 5G, J). However, expression of the *5T4* C-terminal 30 or 40 aa deletion construct (*5T4- Δ C30* or *5T4- Δ C40*) showed a similar level (1.1- and 1.2-fold) of branching numbers in the GC dendrites to that of the control *EYFP*, respectively (Fig. 5H–J). These results indicate that the *5T4*-IC internal domain without the PDZ-binding motif is necessary for the dendritic arborization of GCs.

To test whether the *5T4*-IC domain is sufficient for the dendritic arborization, domain swap experiments were performed with CD8, a TM glycoprotein expressed by a subset of T lympho-

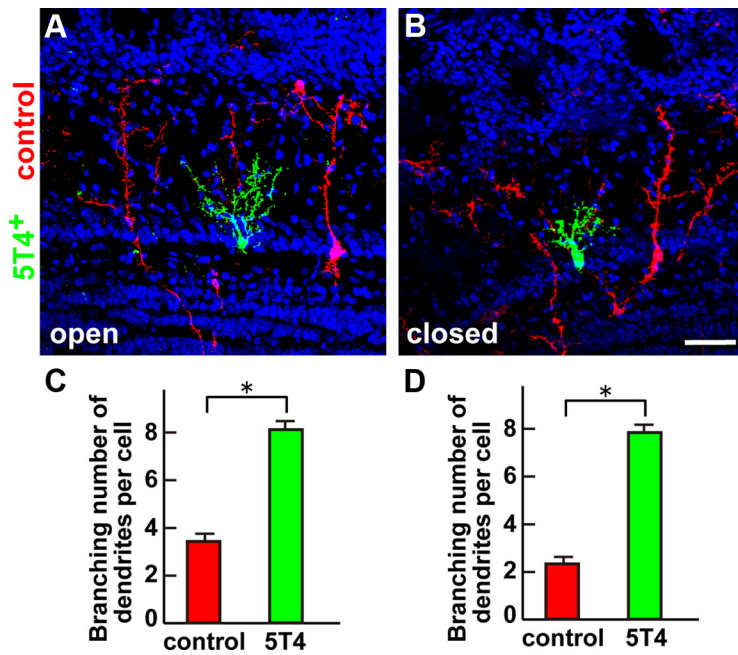


Figure 4. Overexpression of *5T4* restores the dendritic branching of GCs in the closed side of OB. **A, B**, Coinjection of the *5T4*-expressing (*CMVp-5T4-IRES-gapEYFP*) and control (*CMVp-gapmCherry*) lentiviral vectors into the lateral ventricles of naris-occluded mice. The *5T4*-overexpressing GCs ($5T4^+$), where *EYFP* was also positive, are shown as green; the *mCherry*-expressing GCs (control) are shown as red in the open (**A**) and closed (**B**) sides of OB from P14 mice. Scale bar, 50 μm . **C, D**, Quantification of branching numbers of the control (*mCherry*⁺) and *5T4*-overexpressing GC dendrites in the open (**C**) and closed (**D**) sides of OB from P14 mice, shown as the mean \pm SEM (**C**: control = 3.5 ± 0.2 , $5T4 = 8.0 \pm 0.2$; **D**: control = 2.2 ± 0.2 , $5T4 = 7.8 \pm 0.2$; * $p < 0.01$ compared with the control, Student's *t* test, $n = 30$ cells in each side of OB from three individuals). The *5T4*-overexpressing GCs showed increased branching numbers of dendrites, even in the closed side of OB.

cyte. A CD8–*5T4* chimera comprising the CD8-EC+TM and *5T4*-IC domains was generated and injected into P0 lateral ventricles. Ectopic expression of the *CMV* promoter-driven CD8 full length gave a 1.4-fold increase in branching numbers in the GC dendrites, compared with the control *EYFP* (Fig. 6*A, B, D*). By contrast, ectopic expression of the *CMV* promoter-driven CD8–*5T4* chimera gave 3.1-fold more branched dendrites in the GCs than that of the control *EYFP* (Fig. 6*A, C, D*). These results demonstrate that the *5T4*-IC domain is sufficient for the dendritic arborization.

Downregulation of *5T4* leads to reduction of dendritic arborization in endogenous interneurons

To further investigate the influence of *5T4* in the development of the $5T4^+$ GCs, knock-down or dominant-negative lentiviral vectors were used in conjunction with a *5T4* promoter construct to identify interneurons with endogenous *5T4* expression. To evaluate the *5T4* promoter containing a 6 kb region upstream of the initiation codon, the *5T4* promoter (6 kb)-driving *gapEYFP* (*5T4p-gapEYFP*) construct was injected into P0 lateral ventricles, and double immunostained with *EYFP* and *5T4* antibodies at P14. This identified a specific subset of GCs and PGCs, especially in the mitral and superficial GC layers, where *EYFP*⁺ GCs coexpress endogenous *5T4* (Fig. 7*A–C*, arrowheads). We further analyzed the dendritic morphology only for *EYFP*⁺ (endogenous $5T4^+$) in the GCs.

In the *5T4* knockdown studies, we used lentiviral vectors that express three sets of *5T4-shRNAs* under the human *H1* promoter (*H1p-5T4-shRNA*). Both the three *H1p-5T4-shRNAs* and the *5T4p-gapEYFP* vectors were coinjected into P0 lateral ventricles. Interestingly, coexpression of the *5T4-shRNA* and *EYFP* con-

structs gave 2.2-fold fewer branched dendrites in the GCs than that of the control *5T4p-gapEYFP* (Fig. 7*D, E, G*). This result revealed that the *5T4* knockdown leads to reduction of the dendritic arborization of GCs.

Since the *5T4*-IC region is necessary and sufficient for the dendritic arborization of OB interneurons (Figs. 5, 6), overexpression of the *5T4*-IC domain alone without the TM domain could sequester the downstream signaling components and block dendritic branching. A lentiviral vector carrying the *5T4p-5T4-IC-IRES-gapEYFP* gave 1.9-fold fewer branched dendrites than that of the control *gapEYFP* in the $5T4^+$ GCs (Fig. 7*D, F, G*). This is consistent with the *5T4*-IC region acting as a dominant negative for *5T4* function. Thus, two different types of the *5T4* loss-of-function experiments show the reduction of dendritic arborization in the $5T4^+$ granule cells.

We used the *CMV* promoter in *5T4* overexpression studies in Figures 3–6, since this promoter is robust and can label both $5T4^+$ and $5T4^-$ GCs nearby the mitral cell layer. $5T4^+$ GCs have more branched dendrites (>6) by the endogenous *5T4* expression than $5T4^-$ GCs (Fig. 7*D, G*). Thus, the branching numbers of dendrites in the baseline control depend on which GCs [i.e., $5T4^+$ (>6) and $5T4^-$ (~3)] were labeled by the *CMV* promoter. However, with the *5T4* promoter used in Figure 7, we confirmed that *5T4* overexpression facilitates the branching number of dendrites in $5T4^+$ granule cells (Fig. 8*A, B, D*).

The *5T4* EC LRRs were not needed for the dendritic arborization (Fig. 5*B, C, E*). So far, the function of the *5T4*-EC domain and its ligands/interacting partners has not been reported. However, we found that lentiviral expression of *5T4*-EC domain alone resulted in reduction of the branching number of $5T4^+$ GC dendrites (Fig. 8*A, C, D*). Thus, it is possible that the dendritic arborization of OB granule cells may also be influenced by *5T4* functions associated with its extracellular domain.

OB granule cells in *5T4* knock-out mice show reduced dendritic arborization

To further reveal the phenotype of *5T4* loss-of-function in the OB interneurons, we analyzed the $5T4^+$ GCs in *5T4* knock-out mice where the coding region had been replaced by the *lacZ* gene (Southgate et al., 2010). OB sections of the wild-type (+/+), *5T4* heterozygous (+/–), and *5T4*-null (–/–) mice at P14 were immunostained with *5T4* or *LacZ* antibody, respectively. In the null mice, the dendrites of *LacZ*⁺ interneurons seemed to be less extended in the external plexiform layer than those of $5T4^+$ interneurons in the wild-type mice (Fig. 9*A–F*). To confirm this observation, we injected the lentiviral vector carrying *5T4* promoter-driven *gapEYFP* into lateral ventricles of the $5T4^{+/+}$, $5T4^{+/-}$, and $5T4^{-/-}$ mice under the naris-occluded condition. In the open side of OB, $5T4^+$ (*EYFP*⁺) GCs in the heterozygote showed 1.4-fold less dendritic branching than those in the wild type (Fig. 10*A, B, G*), while in

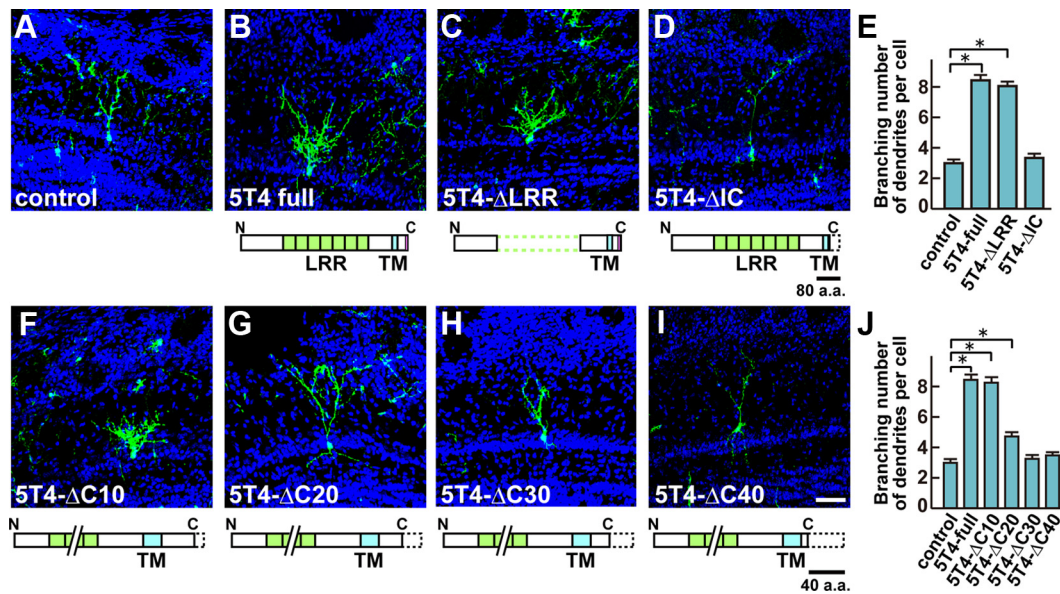


Figure 5. The 5T4 IC region is necessary for the dendritic arborization. *A–E*, 5T4 deletion experiments. Lentiviral vectors carrying the control (*A*), 5T4-full length (*B*), 5T4-ΔLRR (*C*), and 5T4-ΔIC (*D*) regions were injected into P0 mice. Note that the 5T4-IC region is necessary for the dendritic arborization, but the 5T4-LRR domain is not. *E*, Quantification on branching numbers of GC dendrites expressing the control, 5T4-full length or 5T4-deletions in P14 OBs, shown as the mean ± SEM (control = 3.1 ± 0.3, 5T4-full length = 8.2 ± 0.3, 5T4-ΔLRR = 7.9 ± 0.3, 5T4-ΔIC = 3.4 ± 0.2, **p* < 0.01 compared with the control, Student's *t* test, *n* = 30 cells in each type of cells from three individuals). *F–J*, 5T4-IC deletion experiments. Lentiviral vectors carrying a series of 10 aa (*F*), 20 aa (*G*), 30 aa (*H*), and 40 aa (*I*) deletions in the C terminus were injected into P0 mice. Note that the 5T4-IC internal region between 10 and 20 aa in the C-terminal end is needed for the dendritic arborization of GCs. Scale bar, 50 μm. *J*, Quantification on branching numbers of GC dendrites expressing the sequential 5T4-IC deletions in P14 OBs, shown as the mean ± SEM (control = 3.1 ± 0.3, 5T4-full length = 8.2 ± 0.3, 5T4-ΔC10 = 8.1 ± 0.2, 5T4-ΔC20 = 4.5 ± 0.2, 5T4-ΔC30 = 3.4 ± 0.2, 5T4-ΔC40 = 3.6 ± 0.2, **p* < 0.01 compared with the control, Student's *t* test, *n* = 30 cells in each line from three individuals).

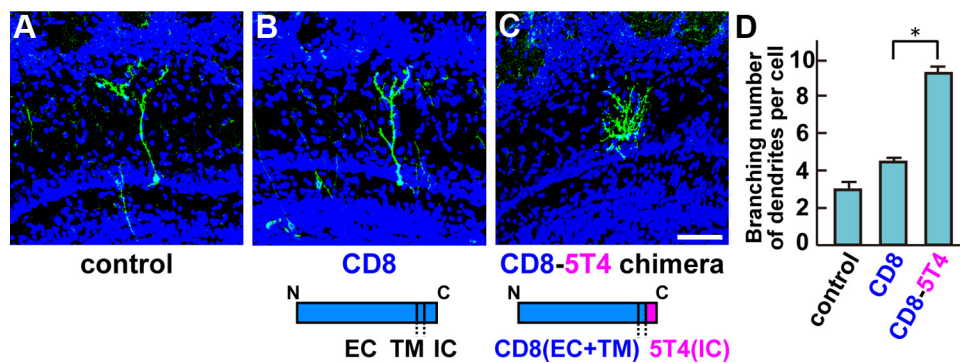


Figure 6. The 5T4 IC region is sufficient for the dendritic arborization. *A–C*, 5T4 domain swap experiments. A lentiviral vector, carrying the control (*A*), CD8 (*B*), or CD8–5T4 chimera (*C*) comprising the CD8 (EC+TM) and 5T4 (IC) domains, was injected into P0 lateral ventricles. Expression of the CD8–5T4 chimera (*C*) in the GCs gives rise to more branched dendrites similar to that seen with the 5T4-full length (Fig. 5*B*). Scale bar, 50 μm. *D*, Quantification on branching numbers of GC dendrites expressing the control, CD8-full length or CD8–5T4 chimera in P14 OBs, shown as the mean ± SEM (control = 2.9 ± 0.2, CD8 = 4.1 ± 0.3, CD8–5T4 fusion = 8.9 ± 0.3, **p* < 0.01 compared with the control, Student's *t* test, *n* = 30 cells in each line from three individuals).

the null mice the dendrites of EYFP⁺ GCs were 2.3-fold less branched than those in the wild type (Fig. 10*A, C, G*). Thus, 5T4 gene dosage appears to correlate with the degree of dendritic arborization. Next, we examined the effect of sensory input on the dendritic branching of 5T4⁺ GCs in the 5T4 mutant mice. In the wild-type mice, the branching number of 5T4⁺ GCs was reduced 1.9-fold under the naris-occluded condition (Fig. 10*A, D, G*), which was consistent with Figure 1. By contrast, the dendritic branching of GCs in the 5T4-null mice showed only slight reduction (1.3-fold) on the closed side than on the open side of OB (Fig. 10*C, F, G*). These results strongly suggest that 5T4 is necessary to regulate the activity-dependent dendritic development of 5T4⁺ granule cells in the OB.

Interestingly, a small number of cell bodies of the 5T4⁺ interneurons was located abnormally at the inner GC layer in the 5T4 heterozygous and null mice (Fig. 9*G–I*). Further, some of these 5T4⁺ interneurons had their dendrites in an irregular rather than a

radially extended orientation. Since the 5T4 gene is expressed in the mitral and the superficial granule cell layers instead of migrating neuroblasts at the RMS, based on *in situ* hybridization and immunostaining, this abnormal positioning of 5T4⁺ interneurons may be derived from a defect of cell migration within OB. These results demonstrate that 5T4 is necessary not only for the dendritic arborization, but may also influence the appropriate positioning of the specific subset of OB interneurons.

Discussion

A DNA microarray and *in situ* hybridization approach identified a trophoblast glycoprotein gene, 5T4, as a candidate gene of OB interneuron development with an expression level that depends on the degree of sensory input. The 5T4 gene is expressed in a specific subset of OB interneurons and is required for their mi-

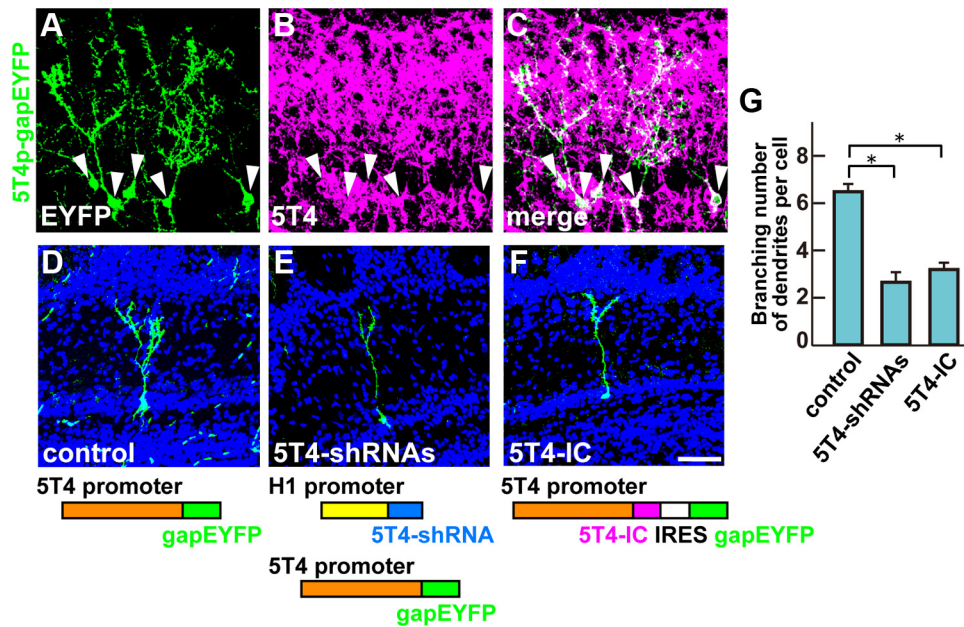


Figure 7. *5T4* knock-down and dominant-negative experiments show reduction of the dendritic arborization in the endogenous cells. **A–C**, The *5T4* promoter analysis. When the *5T4* promoter (6 kb)-driven *gapEYFP* lentiviral vector was injected into the lateral ventricle, *EYFP*⁺ GCs were found at the mitral and granule cell layers in P14 OB (**A**). These *EYFP*⁺ GCs coexpressed the endogenous *5T4* (**A–C**, arrowheads). **D–F**, The *5T4* knockdown and dominant-negative experiments. A lentiviral vector carrying the control (**D**), *5T4*-shRNAs (**E**), or *5T4*-IC (**F**) was injected into P0 lateral ventricles. Expression of the *5T4* shRNAs under the *H1* promoter reduced branching numbers of dendrites in the *5T4*⁺ GCs (**E**) compared with the control (**D**). Likewise, overexpression of the *5T4*-IC region gave fewer branched dendrites in the *5T4*⁺ GCs (**F**). Scale bar, 50 μ m. **G**, Quantification of branching numbers of *5T4*⁺ GC dendrites expressing the control, *5T4*-shRNA, or *5T4*-IC in P14 OBs (control = 6.3 \pm 0.2, *5T4*-RNAi = 2.9 \pm 0.4, *5T4*-DN = 3.4 \pm 0.2, **p* < 0.01 compared with the control, Student's *t* test, *n* = 30 cells in each line from three individuals).

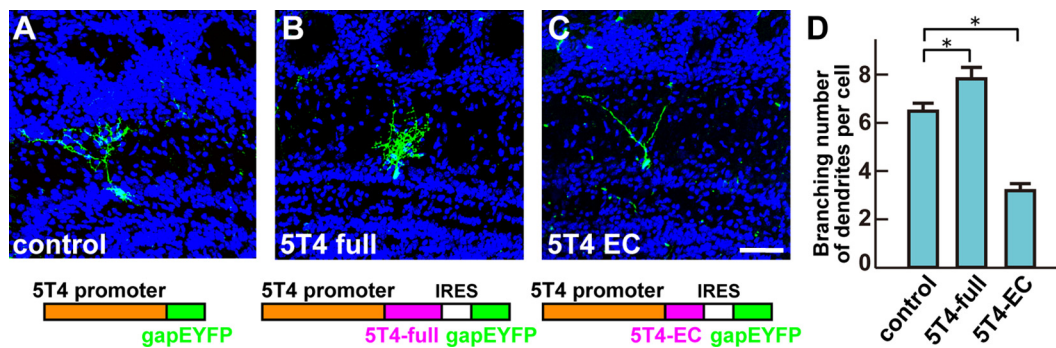


Figure 8. Overexpression of *5T4* EC domain shows reduction of the dendritic arborization in the endogenous cells. **A–C**, Overexpression of *5T4*-full length or *5T4*-EC domain in the endogenous GCs. A lentiviral vector carrying the control (**A**), *5T4*-full length (**B**), or *5T4*-EC (**C**) was injected into P0 lateral ventricles. Expression of the *5T4*-full length under the *5T4* promoter increased branching numbers of dendrites in the *5T4*⁺ GCs (**B**) compared with the control (**A**). In contrast, expression of the *5T4*-EC domain gave fewer branched dendrites in the *5T4*⁺ GCs (**C**) than the control (**A**). Scale bar, 50 μ m. **D**, Quantification of branching numbers of *5T4*⁺ GC dendrites expressing the control, *5T4*-full length or *5T4*-EC in P14 OBs (control = 6.5 \pm 0.4, *5T4*-full length = 7.8 \pm 0.6, *5T4*-EC = 3.2 \pm 0.3, **p* < 0.01 compared with the control, Student's *t* test, *n* = 30 cells in each line from three individuals).

gration/positioning, dendritic arborization following sensory input. Comparative studies of *5T4*^{+/+}, *5T4*^{+/-}, and *5T4*^{-/-} mice showed abnormal phenotypes of both the dendritic branching and the cell positioning of *5T4*⁺ GCs. These results suggest that *5T4* protein in the neurons is necessary for the precise process of the dendritic arborization and cell positioning/migration.

Sensory input regulates the development of adult-born neurons

Sensory input has been classically recognized as important in shaping development and plasticity throughout the nervous system (Katz and Shatz, 1996; Sanes and Lichtman, 2001; Nithianantharajah and Hannan, 2006). In the mouse olfactory epithelium and bulb, sensory input has been studied during development and in adulthood by a variety of manipulations ranging from odor deprivation to genetic silencing of olfactory

sensory neurons (OSNs) (Brunjes, 1994; Zhao and Reed, 2001). Sensory input plays a regulatory role during the OSNs' initial wiring into the glomeruli (Kerr and Belluscio, 2006) as well as in competitive interactions between OSNs as they reinnervate existing glomeruli in adulthood (Zheng et al., 2000; Rochefort et al., 2002; Yamaguchi and Mori, 2005; Imayoshi et al., 2008; Lin et al., 2010; Imamura et al., 2011). In this study, by injecting a lentiviral vector carrying *CMVp-gapEYFP* gene into the lateral ventricle of unilaterally naris-occluded mice, we found that the sensory input is required for the dendritic elongation and arborization in the OB interneurons (Fig. 1). We also found that the *5T4* gain-of-function and loss-of-function lead to facilitation and reduction of dendritic arborization in the OB interneurons, respectively, but not dendritic elongation (Figs. 3, 7). These results suggest that the dendritic arborization of *5T4*⁺ interneurons is augmented in the activated region in OB, where

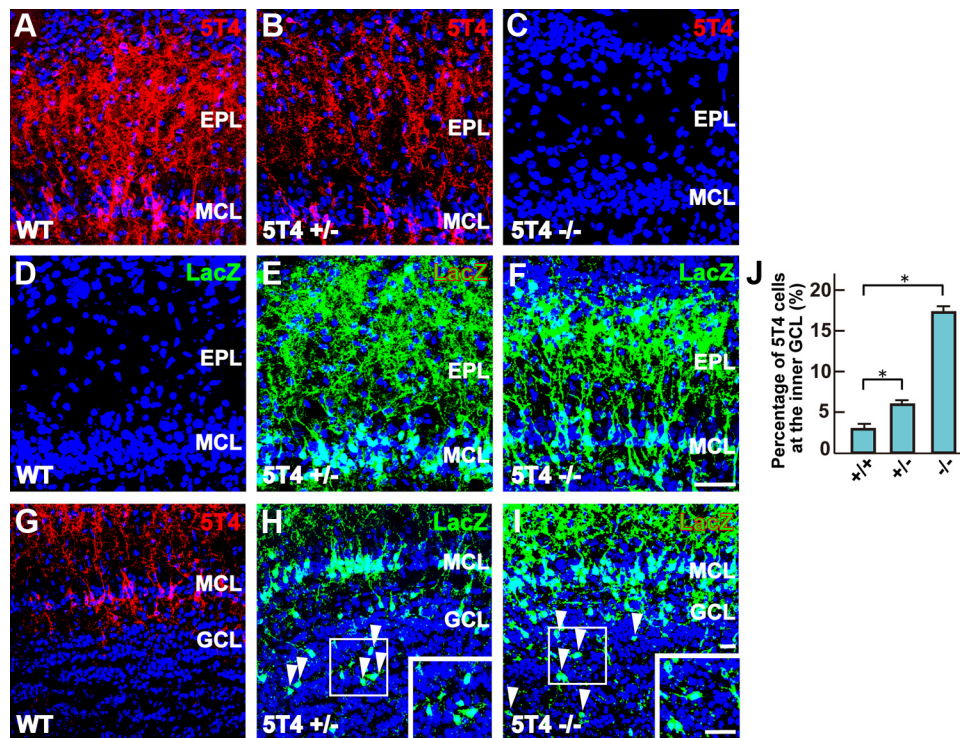


Figure 9. *5T4* knock-out mice show reduction of the dendritic arborization and migration in the corresponding cells. **A–C**, The dendritic arborization of GCs in the *5T4* mutant OBs. OB sections from the WT (+/+), heterozygous (+/-), and null (-/-) mice were immunostained with antibodies against *5T4* (**A–C**) and LacZ (**D–F**), respectively. Scale bar, 50 μ m. **G–I**, The positioning of GCs in the *5T4* mutant OBs. OB sections from the *5T4*^{+/+}, *5T4*^{+/-}, and *5T4*^{-/-} mice were immunostained with antibodies against *5T4* (**G**) and LacZ (**H, I**), respectively. Insets show the enlarged image of the area enclosed with white squares. Scale bar, 20 μ m. Note that a small number of cell bodies of the *5T4*⁺ interneurons were located abnormally at the inner granule cell layer in the both the *5T4*^{+/-} and *5T4*^{-/-} mice (**G–I**, arrowheads). **J**, Quantification on percentages of GCs located abnormally at the inner granule cell layer in the *5T4*^{+/+}, *5T4*^{+/-}, and *5T4*^{-/-} mice in P14 OBs (*5T4*^{+/+} = 2.8 \pm 0.7%, *5T4*^{+/-} = 6.1 \pm 0.4%, *5T4*^{-/-} = 17.8 \pm 0.6%, **p* < 0.01 compared with the wild type, Student's *t* test, data from three individuals in each genotype). EPL, External plexiform layer; MCL, mitral cell layer; GCL, granule cell layer.

the information about abundant odorants in the environment is processed.

How can neural activity in olfactory sensory neurons influence the *5T4* expression in a specific subtype of OB interneurons?

Specific odorant types activate OSNs expressing the appropriate odorant receptors. These neurons project to specific glomeruli in OB and subsequently can activate the specific OB neural circuit locally, upregulating the *5T4* expression level. Our experiments suggest that the increased expression of *5T4* may cause the facilitation of dendritic arborization but not dendritic elongation (Fig. 3). The increased branching numbers of dendrites in *5T4*⁺ interneurons may provide for integrating inputs from a larger receptive field, consistent with the increased *5T4* expression in the OB associated with sensory stimulation. Thus, *5T4*⁺ interneurons that are connected directly or indirectly, via other neurons such as tufted/mitral cells, with glomeruli can be activated by a specific kind of odorants. It is speculated that *5T4* plays an important role in both the complexity and refinement of the OB neural circuitry in an activity-dependent manner.

In cerebral cortex neurons, neural activity is known to induce the elevation of the intracellular calcium ion (Greer and Greenberg, 2008). This calcium elevation activates expression of CAM kinase II and transcription factor CREB. Then, the *CREB* gene activates several genes, including *BDNF* and *c-fos* (Greer and Greenberg, 2008). We recently found that the *5T4* promoter of 6 kb used in this study is downregulated by naris occlusion (data

not shown). The 6 kb region contains putative binding motifs of activity-dependent transcription factors such as *CREB*, *E4BP4*, *c-Ets*, *GATA-1*, *C/EBP α* , *Oct-1*, and other genes (data not shown). Further studies on the 6 kb promoter will lead to elucidating the regulatory mechanism of *5T4* gene expression, depending on the sensory input.

How does *5T4* regulate the dendritic arborization of OB interneurons?

The *5T4* deletion and domain swap experiments established that the *5T4* intracellular domain is necessary and sufficient for the dendritic arborization of GCs (Figs. 5, 6). It was reported that *5T4* overexpression in the mouse fibroblasts or epithelial cells generates a more spindle-shaped morphology, compared with the control cells with affects on the cytoskeleton organization (Carsberg et al., 1995, 1996). The disruption of the cytoskeleton was associated with the *5T4* cytoplasmic domain, and yeast two-hybrid approaches identified several interacting proteins, through the C-terminal PDZ-binding motif (SDV), such as TIP2/GIPC1 (Awan et al., 2002), that interact with α -actinin-1 to stabilize the actin bundles. This type of functional interaction does not appear relevant to the OB interneuron development, since GIPC1 is expressed in mitral cells but not GCs and PGCs (data not shown), and the *5T4*-PDZ binding motif is not necessary for the dendritic arborization of OB interneurons (Fig. 5*F, J*). Further studies are required to identify the mechanisms underlying the influence of the *5T4* intracellular domain on dendritic arborization. Interestingly, we found that lentiviral expression of *5T4* extra-

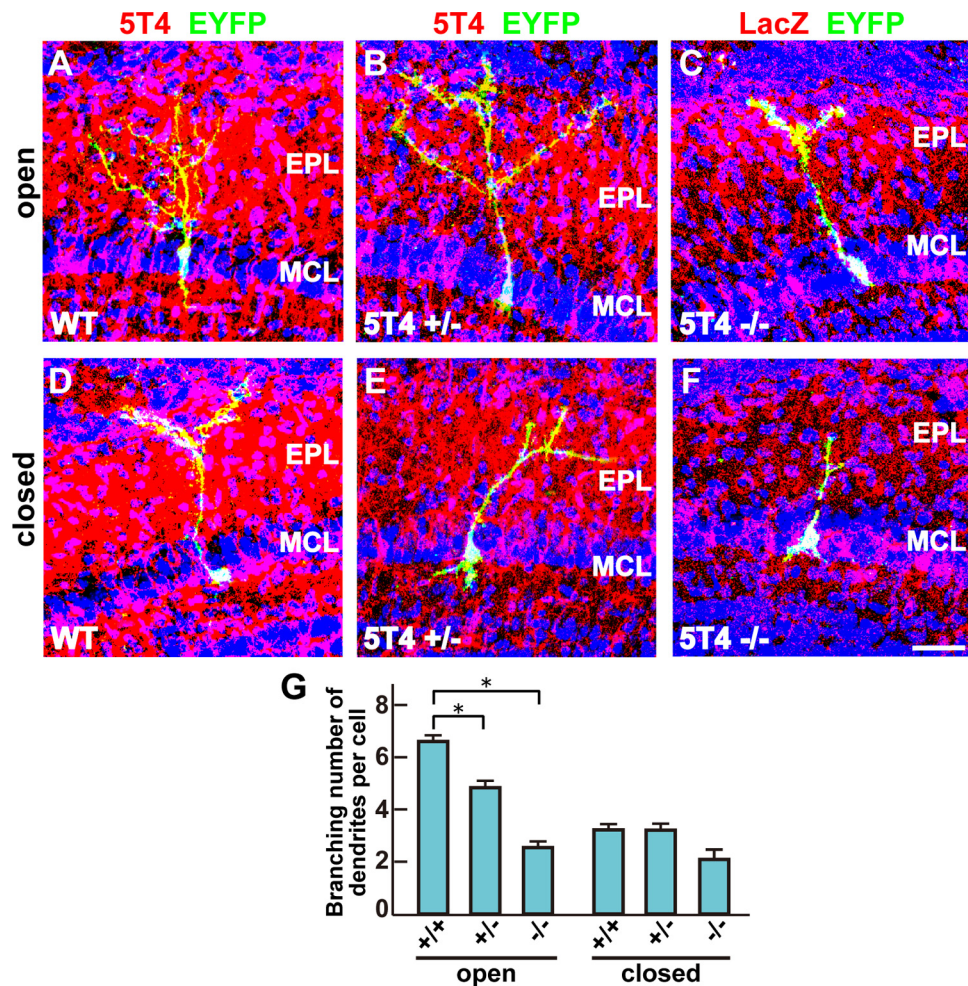


Figure 10. *ST4* knock-out mice show reduction of the dendritic arborization in the corresponding cells. **A–F**, The dendritic arborization of GCs in the *ST4* mutant OBs under the naris-occluded condition. The lentiviral vector carrying *ST4* promoter-driven *gapEYFP* was injected into lateral ventricles of *ST4*^{+/+} (**A, D**), *ST4*^{+/-} (**B, E**), and *ST4*^{-/-} (**C, F**) mice under the naris-occluded condition. Scale bar, 30 μ m. **G**, Quantification on branching numbers of GCs in the *ST4* mutant OBs under the naris-occluded condition (open side: *ST4*^{+/+} = 6.4 \pm 0.5, *ST4*^{+/-} = 4.6 \pm 0.6, *ST4*^{-/-} = 2.8 \pm 0.4; closed side: *ST4*^{+/+} = 3.3 \pm 0.5, *ST4*^{+/-} = 3.1 \pm 0.5, *ST4*^{-/-} = 2.1 \pm 0.4; **p* < 0.01 compared with the wild type, Student's *t* test, data from 10 cells in each genotype). Note that the dendritic branching of GCs was significantly reduced in the *ST4*-null mice compared with the wild type (**A, C, G**). By contrast, the naris occlusion gave only slight reduction of the branching number of GC dendrites in the *ST4*-null mice compared with the wild type (**D, F, G**).

cellular domain alone resulted in reduction of the branching number of *ST4*⁺ GCs (Fig. 8*A, C*). This suggests that *ST4* extracellular domain plays a role in dendritic arborization of OB interneurons via interaction with its ligands.

Cell migration and positioning can also be regulated by the cytoskeleton (Parsons et al., 2010), and in *ST4*-null mice there was evidence of imprecise positioning of *ST4*⁺ interneurons in the OB (Fig. 9). However, such effects were not observed in the behavior of interneurons induced by expression of either the shRNA vectors or the dominant-negative construct. It is possible that these neurons are rescued by the endogenous normal OB microenvironment. Indeed, *ST4* expression is known to facilitate the response to the chemokine CXCL12 through its specific receptor CXCR4, as demonstrated in differentiating mouse embryonic stem cells (Southgate et al., 2010). It is known that CXCR4 regulates cortical interneuron migration and their final laminar positioning (Wang et al., 2011); however, our *in situ* hybridization and immunostaining failed to detect the CXCR4 transcript and product in the *ST4*⁺ OB interneurons (data not shown).

Recently, it has been shown that *ST4* is both induced by and negatively regulates the Wnt canonical pathway, which then

facilitates the response to the noncanonical pathway (Kagermeier-Schenk et al., 2011). Thus, neural activity might induce canonical Wnt ligand production, leading to upregulation of *ST4*, which subsequently blocks the canonical and favors the noncanonical pathway in the unconnected OB interneurons. Importantly, disruption of the *Wnt5a* gene, encoding a noncanonical pathway ligand expressed in a subtype of OB interneurons, gives rise to reduction of the dendritic extension of GCs, compared with the wild type (Pino et al., 2011). It is possible that *Wnt5a* production regulates the non-canonical/planar cell polarization pathways, leading to the facilitation of dendritic arborization (Van Amerongen and Nusse, 2009). Since the *ST4*-IC internal domain, which lacks the PDZ-binding motif, is necessary for the dendritic shaping in *ST4*⁺ GCs (Fig. 5*F, J*), we speculate that it may modulate key interactions that influence Wnt signaling pathways to regulate the dendritic arborization. Identification of proteins that interact with the *ST4* intracellular region will be important on elucidating the mechanisms regulating the dendritic development in OB interneurons, which are likely to include modulation of the cytoskeleton, in the sensory input-dependent manner.

References

- Adam Y, Mizrahi A (2010) Circuit formation and maintenance—perspectives from the mammalian olfactory bulb. *Curr Opin Neurobiol* 20:134–140.
- Awan A, Lucic MR, Shaw DM, Sheppard F, Westwater C, Lyons SA, Stern PL (2002) 5T4 interacts with TIP-2/GIPC, a PDZ protein, with implications for metastasis. *Biochem Biophys Res Commun* 290:1030–1036.
- Barrow KM, Ward CM, Rutter J, Ali S, Stern PL (2005) Embryonic expression of murine 5T4 oncofetal antigen is associated with morphogenetic events at implantation and in developing epithelia. *Dev Dyn* 233:1535–1545.
- Brunjes PC (1994) Unilateral naris closure and olfactory system development. *Brain Res Brain Res Rev* 19:146–160.
- Carsberg CJ, Myers KA, Evans GS, Allen TD, Stern PL (1995) Metastasis-associated 5T4 oncofetal antigen is concentrated at microvillus projections of the plasma membrane. *J Cell Sci* 108:2905–2916.
- Carsberg CJ, Myers KA, Stern PL (1996) Metastasis-associated 5T4 antigen disrupts cell-cell contacts and induces cellular motility in epithelial cells. *Int J Cancer* 68:84–92.
- Eastham AM, Spencer H, Soncin F, Ritson S, Merry CL, Stern PL, Ward CM (2007) Epithelial-mesenchymal transition events during human embryonic stem cell differentiation. *Cancer Res* 67:11254–11262.
- Greer PL, Greenberg ME (2008) From synapse to nucleus: calcium-dependent gene transcription in the control of synapse development and function. *Neuron* 59:846–860.
- Hole N, Stern PL (1990) Isolation and characterization of 5T4, a tumour-associated antigen. *Int J Cancer* 45:179–184.
- Imamura F, Nagao H, Naritsuka H, Murata Y, Taniguchi H, Mori K (2006) A leucine-rich repeat membrane protein, 5T4, is expressed by a subtype of granule cells with dendritic arbors in specific strata of the mouse olfactory bulb. *J Comp Neurol* 495:754–768.
- Imamura F, Ayoub AE, Rakic P, Greer CA (2011) Timing of neurogenesis is a determinant of olfactory circuitry. *Nat Neurosci* 14:331–337.
- Imayoshi I, Sakamoto M, Ohtsuka T, Takao K, Miyakawa T, Yamaguchi M, Mori K, Ikeda T, Itohara S, Kageyama R (2008) Roles of continuous neurogenesis in the structural and functional integrity of the adult forebrain. *Nat Neurosci* 11:1153–1161.
- Inoue M, Nishimura S, Hori G, Nakahara H, Saito M, Yoshihara Y, Amari S (2004) Improved parameter estimation for variance-stabilizing transformation of gene-expression microarray data. *J Bioinform Comput Biol* 2:669–679.
- Kagermeier-Schenk B, Wehner D, Ozhan-Kizil G, Yamamoto H, Li J, Kirchner K, Hoffmann C, Stern P, Kikuchi A, Schambony A, Weidinger G (2011) The transmembrane protein Waif1/5T4 inhibits Wnt/ β -catenin signaling and activates noncanonical Wnt pathways by modifying LRP6 subcellular localization. *Dev Cell* 21:1129–1143.
- Kaneko N, Marín O, Koike M, Hirota Y, Uchiyama Y, Wu JY, Lu Q, Tessier-Lavigne M, Alvarez-Buylla A, Okano H, Rubenstein JL, Sawamoto K (2010) New neurons clear the path of astrocytic processes for their rapid migration in the adult brain. *Neuron* 67:213–223.
- Katz LC, Shatz CJ (1996) Synaptic activity and the construction of cortical circuits. *Science* 274:1133–1138.
- Kelsch W, Lin CW, Mosley CP, Lois C (2009) A critical period for activity-dependent synaptic development during olfactory bulb adult neurogenesis. *J Neurosci* 29:11852–11858.
- Kerr MA, Belluscio L (2006) Olfactory experience accelerates glomerular refinement in the mammalian olfactory bulb. *Nat Neurosci* 9:484–486.
- King KW, Sheppard FC, Westwater C, Stern PL, Myers KA (1999) Organization of the mouse and human 5T4 oncofetal leucine-rich glycoprotein genes and expression in foetal and adult murine tissues. *Biochim Biophys Acta* 1445:257–270.
- Lin CW, Sim S, Ainsworth A, Okada M, Kelsch W, Lois C (2010) Genetically increased cell-intrinsic excitability enhances neuronal integration into adult brain circuits. *Neuron* 65:32–39.
- Livneh Y, Feinstein N, Klein M, Mizrahi A (2009) Sensory input enhances synaptogenesis of adult-born neurons. *J Neurosci* 29:86–97.
- Lledo PM, Merkle FT, Alvarez-Buylla A (2008) Origin and function of olfactory bulb interneuron diversity. *Trends Neurosci* 31:392–400.
- Nithianantharajah J, Hannan AJ (2006) Enriched environments, experience-dependent plasticity and disorders of the nervous system. *Nat Rev Neurosci* 7:697–709.
- Parsons JT, Horwitz AR, Schwartz MA (2010) Cell adhesion: integrating cytoskeletal dynamics and cellular tension. *Nat Rev Mol Cell Biol* 11:633–643.
- Pino D, Choe Y, Pleasure SJ (2011) Wnt5a controls neurite development in olfactory bulb interneurons. *ASN Neuro* 3:e00059.
- Rocheffort C, Gheusi G, Vincent JD, Lledo PM (2002) Enriched odor exposure increases the number of newborn neurons in the adult olfactory bulb and improves odor memory. *J Neurosci* 22:2679–2689.
- Saghatelyan A, Roux P, Migliore M, Rocheffort C, Desmaisons D, Charneau P, Shepherd GM, Lledo PM (2005) Activity-dependent adjustments of the inhibitory network in the olfactory bulb following early postnatal deprivation. *Neuron* 46:103–116.
- Sakamoto M, Imayoshi I, Ohtsuka T, Yamaguchi M, Mori K, Kageyama R (2011) Continuous neurogenesis in the adult forebrain is required for innate olfactory responses. *Proc Natl Acad Sci U S A* 108:8479–8484.
- Sanes JR, Lichtman JW (2001) Induction, assembly, maturation and maintenance of a postsynaptic apparatus. *Nat Rev Neurosci* 2:791–805.
- Southall PJ, Boxer GM, Bagshawe KD, Hole N, Bromley M, Stern PL (1990) Immunohistological distribution of 5T4 antigen in normal and malignant tissues. *Br J Cancer* 61:89–95.
- Southgate TD, McGinn OJ, Castro FV, Rutkowski AJ, Al-Muftah M, Marinov G, Smethurst GJ, Shaw D, Ward CM, Miller CJ, Stern PL (2010) CXCR4 mediated chemotaxis is regulated by 5T4 oncofetal glycoprotein in mouse embryonic cells. *PLoS One* 5:e9982.
- Spencer HL, Eastham AM, Merry CL, Southgate TD, Perez-Campo F, Soncin F, Ritson S, Kemler R, Stern PL, Ward CM (2007) E-cadherin inhibits cell surface localization of the pro-migratory 5T4 oncofetal antigen in mouse embryonic stem cells. *Mol Biol Cell* 18:2838–2851.
- Torashima T, Yamada N, Itoh M, Yamamoto A, Hirai H (2006) Exposure of lentiviral vectors to subneutral pH shifts the tropism from Purkinje cell to Bergmann glia. *Eur J Neurosci* 24:371–380.
- Tsuboi A, Yoshihara S, Yamazaki N, Kasai H, Asai-Tsuboi H, Komatsu M, Serizawa S, Ishii T, Matsuda Y, Nagawa F, Sakano H (1999) Olfactory neurons expressing closely linked and homologous odorant receptor genes tend to project their axons to neighboring glomeruli on the olfactory bulb. *J Neurosci* 19:8409–8418.
- van Amerongen R, Nusse R (2009) Towards an integrated view of Wnt signaling in development. *Development* 136:3205–3214.
- Wang Y, Li G, Stanco A, Long JE, Crawford D, Potter GB, Pleasure SJ, Behrens T, Rubenstein JL (2011) CXCR4 and CXCR7 have distinct functions in regulating interneuron migration. *Neuron* 69:61–76.
- Whitman MC, Greer CA (2009) Adult neurogenesis and the olfactory system. *Prog Neurobiol* 89:162–175.
- Yamaguchi M, Mori K (2005) Critical period for sensory experience-dependent survival of newly generated granule cells in the adult mouse olfactory bulb. *Proc Natl Acad Sci U S A* 102:9697–9702.
- Yoshihara S, Omichi K, Yanazawa M, Kitamura K, Yoshihara Y (2005) Arx homeobox gene is essential for development of mouse olfactory system. *Development* 132:751–762.
- Zhao H, Reed RR (2001) X inactivation of the OCN1 channel gene reveals a role for activity-dependent competition in the olfactory system. *Cell* 104:651–660.
- Zheng C, Feinstein P, Bozza T, Rodriguez I, Mombaerts P (2000) Peripheral olfactory projections are differentially affected in mice deficient in a cyclic nucleotide-gated channel subunit. *Neuron* 26:81–91.